Atmos. Chem. Phys. Discuss., https://doi.org/10.5194/acp-2019-37
Manuscript under review for journal Atmos. Chem. Phys.
Discussion started: 8 March 2019

Atmospheric Chemistry and Physics
Discussions

Historical (1700–2012) Global Multi-model Estimates of the Fire Emissions from the Fire Modeling Intercomparison Project (FireMIP)

Fang Li[1*], Maria Val Martin[2], Stijn Hantson[3,4], Meinrat O. Andreae[5], Almut Arneth[4], Gitta Lasslop[6], Chao Yue[7,8], Dominique Bachelet[9], Matthew Forrest[6], Johannes W. Kaiser[10,5], Erik Kluzek[11], Xiaohong Liu[12], Joe R. Melton[13], Daniel S. Ward[14], Anton Darmenov[15], Thomas Hickler[6,16], Charles Ichoku[17], Brian I. Magi[18], Stephen Sitch[19], Guido R. van der Werf[20], Christine Wiedinmyer[21]

[1] International Center for Climate and Environment Sciences, Institute of Atmospheric Physics, Chinese Academy of Sciences, Beijing, China

[2] Leverhulme Center for Climate Change Mitigation, Department of Animal & Plant Sciences, Sheffield University, Sheffield, UK

[3] Geospatial Data Solutions Center, University of California, Irvine, CA, USA

[4] Karlsruhe Institute of Technology (KIT), Institute of Meteorology and Climate research, Atmospheric Environmental Research, Garmisch-Partenkirchen, Germany

[5] Max Planck Institute for Chemistry, Mainz, Germany

[6] Senckenberg Biodiversity and Climate Research Institute (BiK-F), Senckenberganlage, Germany

[7] Laboratoire des Sciences du Climat et de l'Environnement, LSCE/IPSL, CEA-CNRS-UVSQ, Université Paris-Saclay, Gif-sur-Yvette, France

[8] State Key Laboratory of Soil Erosion and Dryland Farming on the Loess Plateau, Northwest A&F University, Yangling, Shanxi, China

Atmos. Chem. Phys. Discuss., https://doi.org/10.5194/acp-2019-37
Manuscript under review for journal Atmos. Chem. Phys.
Discussion started: 8 March 2019

[9] Biological and Ecological Engineering, Oregon State University, Corvallis, OR, USA

[10] Deutscher Wetterdienst, Offenbach, Germany

[11] National Center for Atmospheric Research, Boulder, CO, USA

[12] Department of Atmospheric Science, University of Wyoming, Laramie, WY, USA

[13] Climate Research Division, Environment and Climate Change Canada, Victoria, BC, Canada

[14] Karen Clark and Company, Boston, MA, USA

[15] Global Modeling and Assimilation Office, NASA Goddard Space Flight Center, Greenbelt, MD, USA

[16] Department of Physical Geography, Goethe University, Frankfurt am Main, Germany

[17] Howard University, NW, Washington, DC, USA

[18] Department of Geography and Earth Sciences, University of North Carolina at Charlotte, Charlotte, NC, USA

[19] College of Life and Environmental Sciences, University of Exeter, Exeter, UK

[20] Faculty of Science, Vrije Universiteit, Amsterdam, The Netherlands

[21] University of Colorado Boulder, Boulder, CO, USA

*Correspondence to: Fang Li (lifang@mail.iap.ac.cn)

Atmos. Chem. Phys. Discuss., https://doi.org/10.5194/acp-2019-37
Manuscript under review for journal Atmos. Chem. Phys.
Discussion started: 8 March 2019

Abstract

Fire emissions are critical for carbon and nutrient cycles, climate, and air quality. Dynamic Global Vegetation Models (DGVMs) with interactive fire modeling provide important estimates for long-term and large-scale changes of fire emissions. Here we present the first multi-model estimates of global gridded historical fire emissions for 1700–2012, including carbon and 33 species of trace gases and aerosols. The dataset is based on simulations of nine DGVMs with different state-of-the-art global fire models that participated in the Fire Modeling Intercomparison Project (FireMIP), using the same and standardized protocols and forcing data, and the most up-to-date fire emission factor table from field and laboratory studies over various land cover types. We evaluate the simulations of present-day fire emissions by comparing them with satellite-based products. Evaluation results show that most DGVMs simulate present-day global fire emission totals within the range of satellite-based products, and can capture the high emissions over the tropical savannas, low emissions over the arid and sparsely vegetated regions, and the main features of seasonality. However, most of the models fail to simulate the interannual variability, partly due to a lack of modeling peat fires and tropical deforestation fires. Historically, all models show only a weak trend in global fire emissions before ~1850s, consistent with multi-source merged historical reconstructions. The long-term trends among DGVMs are quite different for the 20th century, with some models showing an increase and others a decrease in fire emissions, mainly as a result of the discrepancy in their simulated responses to human population density change and land-use and land-cover change

(LULCC). Our study provides a basic dataset for developing regional and global multi-source merged historical reconstructions and merging methods, and analyzing historical changes of fire emissions and their uncertainties as well as their role in the Earth system. It also highlights the importance of accurately modeling the responses of fire emissions to LULCC and population density change in reducing uncertainties in historical reconstructions of fire emissions and providing more reliable future projections.

1. Introduction

Fire is an intrinsic feature of terrestrial ecosystem ecology globally, and has emerged soon after the appearance of terrestrial plants over 400 million years ago (Scott and Glasspool, 2006; Bowman et al., 2009). Fire emissions are a key component of the global and regional carbon budgets (Bond-Lamberty et al., 2007; Ciais et al., 2013; Kondo et al., 2018), and also a major source of greenhouse gases (Tian et al., 2016) and the largest contributor of primary carbonaceous aerosols globally (Andreae and Rosenfeld, 2008; Jiang et al., 2016). By changing the atmospheric composition, fire emissions can have resultant effects on global and regional radiation balance and climate (Ward et al., 2012; Tosca et al. 2013; Jiang et al., 2016; Grandey et al., 2016; McKendry et al., 2018; Hamilton et al., 2018; Thornhill et al., 2018), terrestrial nutrient and carbon cycles (Mahowald et al., 2008; Chen et al., 2010; McKendry et al., 2018; Yue and Unger, 2018), and air quality (Val Martin et al., 2015; Knorr et al., 2017), which is a major human health hazard and has been estimated to result in at least ~165,000, and more likely ~339,000 pre-mature deaths per year globally (Johnston et al., 2012; Marlier et al., 2013; Lelieveld et al., 2015).

To date, only emissions from individual fires or small-scale fire complexes can be directly measured from laboratory experiments and field campaigns (Andreae and Merlet, 2001; Yokelson et al., 2013; Stockwell et al., 2016). Regionally and globally, fire emissions are estimated based on satellite observations, fire proxies, or numerical models. Satellite-based fire emission estimates are derived from satellite observations of burned area, active fire counts, fire radiative power, and/or constrained by satellite observations of aerosol optical depth (AOD), CO, or CO_2 (Wiedinmyer et al., 2011; Kaiser et al., 2012; Krol et al., 2013; Konovalov et al., 2014; Ichoku and Ellison, 2014; Darmenov and da Silva, 2015; van der Werf et al., 2017; Heymann et al., 2017). Data are available globally, but only cover the present-day period. Fire proxies include records of CH_4, black carbon, levoglucosan, ammonium, and CO concentration trapped in the air enclosed in ice cores (Ferretti et al., 2005; McCornnell et al., 2007; Wang et al., 2012; Zennaro et al., 2014), site-level sedimentary charcoal records (Marlon et al., 2008, 2016), visibility records (van Marle et al., 2017a), and aerosol indices (Duncan et al., 2003). These fire proxies cover decades to millennia, but are of limited spatial extent, cannot be directly related to emission amount, and have large uncertainties and discrepancies in their referred regional or global long-term trends due to limited sample size or/and often unclear representative area and time period of fire emissions (Pechony and Shindell, 2010; van der Werf et al., 2013; Legrand et al., 2016).

Atmos. Chem. Phys. Discuss., https://doi.org/10.5194/acp-2019-37
Manuscript under review for journal Atmos. Chem. Phys.
Discussion started: 8 March 2019

Dynamic Global Vegetation Models (DGVMs) that include fire modeling are indispensable for estimating fire carbon emissions at global and regional scales and for past, present, and future periods (Hantson et al., 2016). These models represent interactions among fire dynamics, biogeochemistry, biogeophysics, and vegetation dynamics at the land surface in a physically and chemically consistent modeling framework. DGVMs also constitute the terrestrial ecosystem component of Earth System models (ESMs) and are applied to global change research (Levis et al., 2004; Li et al., 2013; Kloster and Lasslop, 2017). Using fire carbon emissions simulated by DGVMs and fire emission factors, fire emissions of trace gases and aerosols can be derived (Li et al., 2012; Knorr et al., 2016).

Modeling fire and fire emissions within DGVMs started in the early 2000s (Thonicke et al., 2001), and has rapidly progressed during the past decade (Hantson et al., 2016). The Fire Model Intercomparison Project (FireMIP) initiated in 2014 was the first international collaborative effort to better understand the behavior of global fire models (Hantson et al., 2016), where a set of common fire modeling experiments driven by the same forcing data were performed (Rabin et al., 2017). Nine DGVMs with different state-of-the-art global fire models participated in FireMIP. All global fire models used in the upcoming 6^{th} Coupled Model Intercomparison Project (CMIP6) and IPCC AR6 were included in FireMIP, except for the fire scheme in GFDL-ESM (Rabin et al., 2018; Ward et al., 2018) which is similar to that of CLM4.5 (Li et al., 2012) in FireMIP. Furthermore, GlobFIRM (Thonicke et al., 2001) in FireMIP was the most commonly-used fire scheme in CMIP5 (Kloster and Lasslop, 2017).

Earlier studies provided only one single time series of fire emissions for global grids or regions (Schultz et al., 2008; Mieville et al., 2010; Lamarque et al., 2010; Marlon et al., 2016; van Marle et al., 2017b; and references therein), limiting their utility for quantifying the uncertainty in global and regional reconstructions of fire emissions and its subsequent impacts on estimated historical changes in carbon cycle, climate, and air pollution. A small number of studies also investigated the drivers of fire carbon emission trends (Kloster et al., 2010; Yang et al., 2014; Li et al., 2018; Ward et al., 2018). However, because only a single DGVM was used in these studies, they could not identify the uncertainty source in recent model-based reconstructions or help understand the inter-model discrepancy in projections of future fire emissions.

Our study provides a new dataset of global gridded fire emissions, including carbon and 33 species of trace gases and aerosols, over the 1700–2012 time period, based on the nine DGVMs with different state-of-the-art global fire models that participated in FireMIP. The dataset provides the basis for developing multi-source (satellite-based products, model simulations, and/or fire proxies) merged fire emission reconstructions and methods. It also, for the first time, allows end users to select all or a subset of model-based reconstructions that best suits their regional or global research needs, and importantly, to quantify the uncertainty range of past fire emissions and their resulting impacts. In addition, the model-based estimates of fire emissions are comprehensively evaluated through comparison with satellite-based products, including amounts, spatial distribution, seasonality, and interannual variability, providing information on the limitations of recent model-based

Atmos. Chem. Phys. Discuss., https://doi.org/10.5194/acp-2019-37
Manuscript under review for journal Atmos. Chem. Phys.
Discussion started: 8 March 2019

reconstructions. We also analyze long-term trends of the model-based reconstructions, and the forcing drivers of these trends for each DGVM and for inter-model discrepancy.

2 Methods and datasets

2.1 Models in FireMIP

Nine DGVMs with different fire modules participated in FireMIP: CLM4.5 with CLM5 fire module, CTEM, JSBACH-SPITFIRE, JULES-INFERNO, LPJ-GUESS-GlobFIRM, LPJ-GUESS-SIMFIRE-BLAZE, LPJ-GUESS-SPITFIRE, MC2, and ORCHIDEE-SPITFIRE (Table 1, see Rabin et al., 2017 for detailed description of each model). JSBACH, ORCHIDEE, and LPJ-GUESS used the variants of SPITFIRE (Thonicke et al., 2010) with updated representation of human ignitions and suppression, fuel moisture, combustion completeness, and the relationship between spread rate and wind speed for JSBACH (Lasslop et al., 2014), combustion completeness for ORCHIDEE (Yue et al., 2014, 2015), and human ignition, post-fire mortality factors, and modifications for matching tree age/size structure for LPJ-GUESS (Lehsten et al., 2009; Rabin et al., 2017).

The global fire models in the nine DGVMs have diverse levels of complexity (Rabin et al., 2017). SIMFIRE is a statistical model based on present-day satellite-based fire products (Knorr et al., 2016). In CLM4.5, crop, peat, and tropical deforestation fires are empirically/statistically modeled (Li et al., 2013). The scheme for fires outside the tropical closed forests and croplands in CLM4.5 (Li et al., 2012;

Li and Lawrence, 2017) and fire modules in CTEM (Arora and Boer, 2005; Melton and Arora, 2016), GlobFIRM (Thonicke, 2001), and INFERNO (Mangeon et al., 2016) are process-based and of intermediate-complexity. That is, area burned is determined by two processes: fire occurrence and fire spread, but with simple empirical/statistical equations for each process. Fire modules in MC2 (Bachelet et al., 2015; Sheehan et al., 2015) and SPITFIRE variants are more complex, which use the Rothermel equations (Rothermel, 1972) to model fire spread and consider the impact of fuel composition on fire behavior.

The way in which humans affect fire is treated differently among these global fire models (Table 1), influencing the simulations of fire emissions. GlobFIRM does not consider any direct human effect on fires, and MC2 fire model only considers human suppression on fire. CLM4.5 includes crop fires, fires caused by man-made deforestation in tropical closed forests, and human ignitions and suppression on both fire occurrence and spread area for fires outside tropical closed forests and croplands. Burned area in SIMFIRE and human influence on fire occurrence in other models are a non-linear function of population density. CTEM and JSBACH-SPITFIRE also consider human suppression on fire duration. All models, except for CLM4.5, set burned area zero over cropland. Models treat pasture fires as natural grassland fires by using the same parameter values if they have pasture plant functional types (PFTs) or lumping pastures with natural grasslands otherwise. Note that biomass harvest is considered in pastures in LPJ-GUESS-GlobFIRM and

LPJ-GUESS-SIMFIRE-BLAZE, which decreases fuel availability for fires, and that JSBACH-SPITFIRE sets high fuel bulk density for pasture PFTs.

Only CLM4.5 simulates peat fires, although only emissions from burning of vegetation tissues and litter are included in outputs for FireMIP (i.e. burning of soil organic matter is not included).

In the FireMIP models, fire carbon emissions are calculated as the product of burned area, fuel load, and combustion completeness. Combustion completeness is the fraction of live plant tissues and ground litter burned (0.0–1.0). It depends on PFT and plant tissue type in GlobFIRM and in the fire modules of CLM4.5 and CTEM, and also a function of soil moisture in INFERNO. Combustion completeness depends on plant tissue type and surface fire intensity in SIMFIRE, fuel type and wetness in the SPITFIRE family models, and fuel type, load, and moisture in MC2 fire module.

2.2 FireMIP experimental protocol and input datasets

Fire emissions in this study are estimated using the model outputs of PFT-level fire carbon emissions and vegetation characteristics (PFTs and their fractional area coverages) from the FireMIP historical transient control run (SF1) (Rabin et al., 2017). SF1 includes three phases (Fig. 1): the 1700 spin-up phase, the 1701–1900 transient phase, and the 1901–2012 transient phase. In the 1700 spin-up phase, all models are spun up to equilibrium, forced by population density and prescribed land-use and land-cover change (LULCC) at their 1700 values, 1750 atmospheric CO_2 concentration, and the repeatedly cycled 1901–1920 atmospheric forcing

Atmos. Chem. Phys. Discuss., https://doi.org/10.5194/acp-2019-37
Manuscript under review for journal Atmos. Chem. Phys.
Discussion started: 8 March 2019

(precipitation, temperature, specific humidity, surface pressure, wind speed, and solar radiation) and lightning data. The 1701–1900 transient phase is forced by 1701–1900 time-varying population and LULCC, with constant CO_2 concentration at 1750 level until 1750 and time-varying CO_2 concentration for 1750–1900, and the cycled 1901–1920 atmospheric forcing and lightning data. In the 1901–2012 transient phase, models are driven by 1901–2012 time-varying population density, LULCC, CO_2 concentration, atmospheric forcing, and lightning data. Unlike all other models, MC2 and CTEM run from 1901 and 1861, respectively, rather than 1700.

The nine DGVMs are driven with the same forcing data (Rabin et al., 2017). The atmospheric forcing is from CRU-NCEP v5.3.2 with a spatial resolution of 0.5° and a 6-hourly temporal resolution (Wei et al., 2014). The 1750–2012 annual global atmospheric CO_2 concentration is derived from ice core and NOAA monitoring station data (Le Quéré et al., 2014). Annual LULCC and population density at a 0.5° resolution for 1700–2012 are from Hurtt et al. (2011) and Klein Goldewijk et al. (2010, HYDE v3.1), respectively. Monthly cloud-to-ground lightning frequency for 1901–2012, at 0.5° resolution, is derived from the observed relationship between present-day lightning and convective available potential energy (CAPE) anomalies (Pfeiffer et al., 2013, J. Kaplan, personal communication, 2015).

Six FireMIP models (CLM4.5, JSBACH-SPITFIRE, JULES-INFERNO, LPJ-GUESS-SPITFIRE, LPJ-GUESS-SIMFIRE-BLAZE, and ORCHIDEE-SPITFIRE) also provide outputs of five sensitivity simulations: constant climate, constant atmospheric CO_2 concentration, constant land cover, constant population density, and constant lightning frequency throughout the whole simulation period. The sensitivity simulations are helpful for understanding the drivers of changes in reconstructed fire emissions.

2.3 Estimates of fire trace gas and aerosol emissions

Based on fire carbon emissions and vegetation characteristics from DGVMs and fire emission factors, fire emissions of trace gas and aerosol species i and the PFT j, $E_{i,j}$ (g species m^{-2} s^{-1}), are estimated according to Andreae and Merlet (2001):

$$E_{i,j} = \mathrm{EF}_{\mathrm{i,j}} \times CE_j/[\mathrm{C}], \quad (1)$$

where $\mathrm{EF}_{\mathrm{i,j}}$ (g species (kg dry matter (DM)) $^{-1}$) is a PFT-specific emission factor (EF), CE_j denotes the fire carbon emissions of PFT j (g C m^{-2} s^{-1}), and [C]=0.5×10^3 g C (kg DM)$^{-1}$ is a unit conversion factor from carbon to dry matter.

The EFs used in this study (Table 2) are based on Andreae and Merlet (2001), with updates from field and laboratory studies over various land cover types published during 2001–2018 (see Andreae (2019) for details). The EFs are used for all simulations of FireMIP models in the present study.

DGVMs generally simulate vegetation as mixture of PFTs in a given grid location to represent plant function at global scale, instead of land cover types. In Table 3, we associate the PFTs from each DGVM to the land cover types shown in Table 2. Grass, shrub, savannas, woodland, pasture, tundra PFTs are classified as grassland/savannas; tree PFTs as forests and crop PFTs as cropland, similar to Li et al. (2012), Mangeon et al. (2016), and Melton and Arora (2016). PFTs of other broadleaf deciduous tree in CTEM, extra-tropical evergreen and deciduous tree in JSBACH, and broadleaf deciduous tree and needleleaf evergreen tree in JULES are divided into tropical, temperate, and boreal groups following Nemani and Running (1996).

We provide two versions of fire emission products with different spatial resolutions: the original spatial resolution for each FireMIP DGVM outputs (Table 1), and a 1x1 degree horizontal resolution. For the latter, fire emissions are unified to 1 degree resolution using bilinear interpolation for CLM4.5, CTEM, JSBACH, and JULES which have coarser resolution, and area-weighted averaging-up for other models whose original resolution is 0.5 degree. The 1x1 degree product is used for present-day evaluation and historical trend analyses in Sects. 3 and 4.

2.4 Benchmarks

Satellite-based products are commonly used as benchmarks to evaluate present-day fire emission simulations (Rabin et al., 2017, and references therein). In the present study, six satellite-based products are used (Table 4). Fire emissions in GFED4/GFED4s (small fires included in GFED4s) (van der Werf et al., 2017), GFAS1 (Kaiser et al., 2012), and FINN1.5 (Wiedinmyer et al., 2011) are based on EF and CE (Eq. 1). CE is estimated from MODIS burned area and VIRS/ATSR active fire products in the GFED family, MODIS active fire detection in FINN1.5, and MODIS fire radiative power (FRP) in GFAS1. Fire emissions from FEER1 (Ichoku and Ellison, 2014) and QFEDv2.5 (Darmenov and da Silva, 2015) are derived using FRP, and constrained with satellite AOD observations. Satellite-based present-day fire emissions for the same region can differ by a factor of 2–4 on an annual basis (van der Werf et al., 2010) and up to 12 on a monthly basis (Zhang et al., 2014). The discrepancy among them mainly comes from the satellite observations used, the methods applied for deriving fire emissions, and emissions factors.

2.5 Multi-source merged historical reconstruction

We also compared the simulated historical changes with historical reconstructions merged from multiple sources used as forcing data for CMIPs. Fire emission estimates for CMIP5 and CMIP6 were merged from different sources (Table 4). For CMIP5 (Lamarque et al., 2010), the decadal fire emissions are available from 1850 to 2000, estimated using GFED2 fire emissions (van der Werf et al., 2006) for 1997 onwards, RETRO (Schultz et al., 2008) for 1960–1900, GICC (Mieville et al., 2010) for 1900-1950, and kept constant at the 1900 level for 1850–1900. RETRO combined literature reviews with satellite-based fire products and the GlobFIRM fire model. GICC is based on a burned area reconstruction from literature review and sparse tree ring records (Mouillot et al., 2005), satellite-based fire counts, land cover map, and representative biomass density and burning efficiency of each land cover type.

For CMIP6, monthly fire emission estimates are available from 1750 to 2015 (van Marle et al., 2017b). The CMIP6 estimates are merged from GFED4s fire carbon emissions for 1997 onwards, charcoal records GCDv3 (Marlon et al., 2016) for North America and Europe, visibility records for Equatorial Asia (Field et al., 2009) and central Amazon (van Marle et al., 2017b), and the median of six FireMIP models

(CLM4.5, JSBACH-SPITFIRE, JULES-INFERNO, LPJ-GUESS-SPITFIRE, LPJ-GUESS-SIMFIRE-BLAZE, and ORCHIDEE-SPITFIRE) for all other regions. Then, based on the merged fire carbon emissions, CMIP6 fire trace gas and aerosols emissions are derived using EF from Andreae and Merlet (2001) with updates to 2013 and Akagi et al. (2011) with updates for temperate forests to 2014, and a present-day land cover map.

3 Evaluation of present-day fire emissions

The spatial pattern and temporal variability of different fire emission species are similar, with slight discrepancies resulting from the estimated fire carbon emissions over the land cover types that have different emission factors (Table 2). Therefore, we focus on several important species as examples to exhibit the performance of FireMIP models on the simulations of present-day fire emissions.

3.1 Global amounts and spatial distributions

As shown in Table 5, FireMIP models, except for MC2 and LPJ-GUESS-GlobFIRM, estimate present-day fire carbon, CO_2, CO, CH_4, BC, OC, and $PM_{2.5}$ annual emissions to be within the range of satellite-based products. For example, the estimated range of fire carbon emissions is 1.7–3.0 Pg C yr^{-1}, whereas they are 1.5–4.2 Pg C yr^{-1} for satellite-based products. Low fire emissions in MC2 result from relatively low simulated global burned area, only about 1/4 of satellite-based observations (Andela et al., 2017), whereas high emissions in LPJ-GUESS-GlobFIRM are mainly due to the higher combustion completeness of woody tissues (50-90% of stem and coarse woody debris burned in post-fire regions) than those used in other FireMIP models (Rabin et al., 2017) and the satellite-based GFED family (van der Werf et al., 2017).

FireMIP DGVMs, except for MC2, represent the general spatial distribution of fire emissions evident in satellite-based products, with high fire BC emissions over tropical savannas and low emissions over the arid and sparsely vegetated regions (Fig. 2). Among the nine models, CLM4.5, JULES-INFERNO, and LPJ-GUESS-SIMFIRE-BLAZE have higher global spatial pattern correlation with satellite-based products than the other models, indicating higher skill in their spatial-pattern simulations. It should also be noted that, on a regional scale, CTEM, JULES-INFERNO, LPJ-GUESS-SPITFIRE, and ORCHIDEE-SPITFIRE underestimate fire emissions over boreal forests in Asia and North America. LPJ-GUESS-GlobFIRM and LPJ-GUESS-SIMFIRE-BLAZE overestimate fire emissions over the Amazon and African rainforests. CLM4.5 and JSBACH-SPITFIRE overestimate fire emissions over eastern China and North America, respectively. MC2 underestimates fire emissions over most regions, partly because it allows only one ignition per year per grid cell and thus underestimates the burned area.

We further analyze the spatial distribution of inter-model difference. As shown in Fig. 3, the main disagreement among FireMIP models occurs in the tropics, especially over the tropical savannas in Africa, South America, and northern Australia.

Atmos. Chem. Phys. Discuss., https://doi.org/10.5194/acp-2019-37
Manuscript under review for journal Atmos. Chem. Phys.
Discussion started: 8 March 2019

3.2 Seasonal cycle

FireMIP models reproduce similar seasonality features of fire emissions to satellite-based products, that is, peak month is varied from the dry season in the tropics to the warm season in the extra-tropics (Fig. 4).

For the tropics in the Southern Hemisphere, fire PM2.5 emissions of satellite-based products peak in August–September. Most FireMIP models can reproduce this pattern, except ORCHIDEE-SPITFIRE and LPJ-GUESS-SPITFIRE peaking two months and one month earlier, respectively, and JSBACH-SPITFIRE with much lower amplitude of seasonal variability.

For the tropics in the Northern Hemisphere, most FireMIP models exhibit larger fire emissions in the northern winter, consistent with the satellite-based products.

In the northern extra-tropical regions, satellite-based products show two periods of high values: April–May resulting mainly from fires over croplands and grasslands, and July mainly due to fires over the boreal evergreen forests. Most FireMIP models can reproduce the second one, except for LPJ-GUESS-SPITFIRE which peaks in October. CLM4.5 is the only model that can captures both peak periods.

3.3 Interannual variability

Global fire $PM_{2.5}$ emissions from satellite-based products for 1997–2012 show a substantial interannual variability, which peaks in 1997–1998, followed by a low around 2000 and a decline starting in 2002/2003 (Fig. 5). The 1997–1998 high emission values are caused by peat fires in Equatorial Asia in 1997 and widespread drought-induced fires in 1998 associated with the most powerful 1997–1998 El Niño event recorded in history (van der Werf et al., 2017; Kondo et al., 2018). Most FireMIP models cannot reproduce the 1997–1998 peak, except CLM4.5 as the only model that simulates the burning of plant-tissue and litter from peat fires (although burning of soil organic matter is not included) and the drought-linked tropical deforestation and degradation fires (Li et al., 2013, Kondo et al., 2018). CLM4.5, CTEM, and LPJ-GUESS-SIMFIRE-BLAZE present the highest temporal correlation between models and satellite-based products (0.55–0.79 for CLM4.5, 0.51–0.68 for CTEM, and 0.39–0.72 for LPJ-GUESS-SIMFIRE-BLAZE), and thus are more skillful than other models to reproduce the interannual variability observed from satellite-based products (Table 6).

We use the coefficient of variation (CV, the standard deviation divided by the mean, %) to represent the amplitude of interannual variability of fire emissions. As shown in Fig. 5, for 1997–2012, all FireMIP models underestimate the variation as a result of (at least) partially missing the 1997–1998 fire emission peak. For 2003–2012 (the common period of all satellite-based products and models), interannual variation of annual fire $PM_{2.5}$ emissions in CLM4.5, CTEM, and LPJ-GUESS family models lies within the range of satellite-based products (CV=6–12%). Other models present weaker variation (CV=5%) except for MC2 (CV=24%) that has a much stronger variation than all satellite-based products and other FireMIP models.

Atmos. Chem. Phys. Discuss., https://doi.org/10.5194/acp-2019-37
Manuscript under review for journal Atmos. Chem. Phys.
Discussion started: 8 March 2019

4 Historical changes

4.1 Historical changes and drivers

Figure 6 shows historical simulations of the FireMIP models and the CMIP reconstructions for fire carbon, CO_2, CO and $PM_{2.5}$ species. We find similar historical changes for all the species, with the maximum global fire emissions given by LPJ-GUESS-GlobFIRM and the minima by LPJ-GUESS-SPITFIRE before 1901 and MC2 afterwards.

Long-term trends in modelled global fire emissions for all models are weak before the1850s (relative trend <0.015% yr^{-1}), similar to CMIP6 estimates (Fig. 6).

After the1850s, disagreement in the trends among FireMIP models begins to emerge. Fire emissions in LPJ-GUESS-SIMFIRE-BLAZE decline since ~1850, while fire emissions in LPJ-GUESS-SPITFIRE, MC2, and ORCHIDEE-SPITFIRE show upward trends from ~1900s. In CLM4.5, CTEM, and JULES-INFERNO, fire emissions increase slightly before ~1950, similar to the CMIP6 estimates, but CTEM and JULES-INFERNO decrease thereafter, contrary to CMIP5 and CMIP6 estimates and CLM4.5. JSBACH-SPITFIRE simulates a decrease of fire emissions before 1940s and an increase later, similar to the CMIP5 estimates. All the long-term trends described above are significant at the 0.05 level using the Mann-Kendall trend test.

Six FireMIP models also conducted sensitivity experiments, which can be used to identify the drivers of their long-term trends during the 20th century. As shown in Figs. 6 and 7, the downward trend of LPJ-GUESS-SIMFIRE-BLAZE is mainly caused by LULCC and increasing population density. Upward trends in

LPJ-GUESS-SPITFIRE and ORCHIDEE-SPITFIRE are dominated by LULCC and rising population density and CO_2 during the 20th century. In CLM4.5 and JULES-INFERNO, upward trends before ~1950 are attributed to rising CO_2, climate change, and LULCC, and the subsequent drop in JULES-INFERNO mainly results from the rising population density and climate change. Long-term changes in JSBACH-SPITFIRE are mainly driven by LULCC and rising CO_2.

4.2 Drivers for difference in simulated long-term changes

The discrepancy in long-term trends among FireMIP models mainly arises from the simulated anthropogenic influence (LULCC and population density change) on fire emissions (Fig. 7), as the standard deviation in simulated responses to LULCC (0.27 Pg C yr^{-1}) and population density (0.11 Pg C yr^{-1}) is much larger than the other drivers.

LULCC decreases fire emissions sharply in LPJ-GUESS-SIMFIRE-BLAZE during the 20th century, but increases fire emissions for the other models except for JSBACH-SPITFIRE. The response to LULCC in LPJ-GUESS-SIMFIRE-BLAZE is because it assumes no fire in croplands and accounts for biomass harvest (decreases fuel availability) in pastures (Table 1), the area of which expanded over the 20th century. The LULCC-induced increase in fire emissions for the other models are partly caused by increased burned area due to the expansion of grassland (pastures are lumped in grassland in these models) which burn much more easily than woody vegetation in the setup of all FireMIP models (Rabin et al., 2017). Additionally, CLM4.5 models crop fires, which are estimated to increase during the 20th century. JSBACH shifts the sign of response to LULCC around ~1940s due to both assuming no fires over croplands and setting high fuel bulk density for pastures.

Rising population density throughout the 20th century decreases fire emissions in CLM4.5 and LPJ-GUESS-SIMFIRE-BLAZE because they include human suppression on both fire occurrence and fire spread. Fire suppression increases with rising population density simulated explicitly in CLM4.5 and implicitly in LPJ-GUESS-SIMFIRE-BLAZE. On the contrary, rising population density increases fire emissions in LPJ-GUESS-SPITFIRE and ORCHIDEE-SPITFIRE because observed human suppression on fire spread found in Li et al. (2013), Hantson et al. (2015), and Andela et al. (2017) is not taken into account in the two models. The response to population density change for the other models is small, reflecting the compensating effects of human ignition and human suppression on fire occurrence (strongest in JULES-INFERNO in FireMIP models), and human suppression on fire duration (JSBACH-SPITFIRE).

All models simulate increased fire emissions with increased CO_2 since elevated CO_2 increases fuel load through increasing the carbon entering into the land ecosystems (Mao et al., 2009) and improving the water-use efficiency (Keenan et al., 2013). Such a CO_2-driven increase of fuel load is consistent with a recent analysis of satellite-derived vegetation indices (Zhu et al., 2016). FireMIP models also agree that impacts of changes in lightning frequency on long-term trends of fire emissions are small. Moreover, most FireMIP models agree that climate change tends to increase

Atmos. Chem. Phys. Discuss., https://doi.org/10.5194/acp-2019-37
Manuscript under review for journal Atmos. Chem. Phys.
Discussion started: 8 March 2019

fire carbon emissions during the first several decades and then falls, reflecting co-impacts of climate on both fuel load and fuel moisture.

4.3 Regional long-term changes

We divided the global map into regions following the definition of the GFED family (Fig. 8a). As shown in Fig. 8b, inter-model discrepancy in long-term changes are largest in Southern Hemisphere South America (SHSA), southern and northern Africa (NHAF and SHAF), and central Asia (CEAS). In other regions, long-term changes of most FireMIP models are small, similar to CMIP5 or CMIP6 fire emission estimates, except for equatorial Asia where only CLM4.5 partly reproduces the upward trend shown in CMIP5 and CMIP6 estimates after 1950s (not shown).

Most FireMIP models reproduce the upward trends found also in the CMIP5 or CMIP6 estimates since 1950s in SHSA and till ~1950 in Africa (Figs. 9a and b). Long-term trends in regional fire emissions in SHSA, Africa, and central Asia can broadly explain the upward trends in global fire emissions in LPJ-GUESS-SPITFIRE, MC2, and ORCHIDEE-SPITFIRE, the downward trends in LPJ-GUESS-SIMFIRE-BLAZE, and the rise followed by a drop in CTEM, whose global fire emissions exhibit most obvious long-term trends in FireMIP models (Fig. 6).

5 Summary and outlook

Atmos. Chem. Phys. Discuss., https://doi.org/10.5194/acp-2019-37
Manuscript under review for journal Atmos. Chem. Phys.
Discussion started: 8 March 2019

Atmospheric Chemistry and Physics
Open Access
Discussions

Our study provides new multi-model reconstructions of global historical fire emissions for 1700–2012, including carbon and 33 species of trace gases and aerosols. Two versions of the fire emission product are available, at the original spatial resolution for outputs of each FireMIP model and at a unified 1x1 degree. The dataset is based on simulations of fire carbon emissions and vegetation distribution from nine DGVMs with state-of-the-art global fire models that participated in FireMIP and the most up-to-date emission factors over various land cover types. It will be available to the public at https://bwfilestorage.lsdf.kit.edu/public/projects/imk-ifu/FireMIP/emissions.

Our study provides an important dataset with wide-ranging applications for the fire and Earth science research communities. First, it is the best multi-model-based reconstruction of fire emissions so far and for the next several years, and can serve as the basis for further developing multi-source merged products of global and regional fire emissions and the merging methodology. van Marle et al. (2017b) presented an example for using part of the dataset to develop a multi-source merged fire emission product as forcing dataset for CMIP6. In van Marle et al. (2017b), the median of fire carbon emissions from six FireMIP models was used to determine historical changes over most regions of the world. The merging method and merged product in van Marle et al. (2017b) are still preliminary, and need to be improved in the future, e.g. by weighting the different models depending on their global or regional simulation skills. Secondly, our dataset includes global gridded reconstructions for 300 years, thus can be used for analyzing global and regional historical changes in fire emissions on inter-annual to multi-decadal time scales and their interplay with climate variability and human activities. Third, the fire emission reconstructions based on multiple models provide, for the first time, a chance to quantify and understand the uncertainties in historical changes of fire emissions and their subsequent impacts on carbon cycle, radiative balance, air quality, and climate. Hamilton et al. (2018), for example, using fire emission simulations from two global fire models and the CMIP6 estimates to drive an aerosol model, quantified the impact of uncertainties in pre-industrial fire emissions in estimated pre-industrial aerosol concentrations and historical radiative forcing.

This study also provides significant information of the recent state of fire model performance by evaluating the present-day estimates based on FireMIP fire models (also those used in the upcoming CMIP6). Our results show that most FireMIP models can overall reproduce the amount, spatial pattern, and seasonality of fire emissions shown by satellite-based fire products, but fail to simulate the interannual variability partly due to a lack of modeling peat and tropical deforestation fires. In addition, Teckentrup et al. (in prep.) found that climate greatly affected interannual variability of burned area partly through affecting fire duration. However, all FireMIP models limit their fire duration of individual fire events within one day over natural vegetation regions, so they cannot skillfully model the drought-induced large fires that last multiple days (Le Page et al., 2015; Ward et al., 2018). Recently, Andela et al. (2018) derived a dataset of fire duration from MODIS satellite observations, which provided a valuable dataset for developing parameterization of fire duration in global fire models.

This study also identifies population density and LULCC as the primary uncertainty sources in fire emission estimates. Therefore, accurately modeling these responses remains a top priority to reduce uncertainty in historical reconstructions and future projections of fire emissions, especially given that modeling is the only way for future projections. For the response to changes in population density, many FireMIP models have not included the observed relationship between population density and fire spread (Table 1). Moreover, Bistinas et al. (2014) and Parisien et al. (2016) reported obvious spatial heterogeneity of the population density–burned area relationship that is poorly represented in FireMIP models.

For the response to LULCC, improving the modeling of crop and pasture fires and human indirect effect on fires (e.g. fragmentation of the landscape) is critical. Earlier studies reported that the timing and emissions from crop fires were different from natural vegetation fires, and that crop fires could be an important source of greenhouse gas and air pollutant emissions (Magi et al., 2012; Tian et al., 2016; Wu et al., 2017). In FireMIP, only CLM4.5 simulates crop fires, whereas the other models assume no fire over croplands. For pasture fires, all FireMIP models assume that they are as natural grassland fires and this needs to be verified by, for example, satellite-based products. If fires over pastures and natural grasslands are significantly different, adding the gridded coverage of pasture as a new input field in DGVMs without pasture PFTs and developing a parameterization of pasture fires will be necessary. In addition, Archibald (2016) and Andela et al. (2017) found that expansion of croplands and pastures decreased fuel continuity and thus reduced burned area and fire emissions. However, no FireMIP model parameterizes this indirect human effect on fires.

Author contribution. FL contributed to the processing and analyses of the fire emission dataset. SS and AA designed the FireMIP experiments and LF, SH, GL, CY, DB, MF, JM, and TH performed FireMIP simulations. MA compiled the EF table. JK, AD, CI, Gv, CW provided satellite-based and CMIP estimates of fire emissions. FL prepared the first draft of manuscript, and revised it with contributions from all co-authors.

Acknowledgements. This study is co-supported by the National Key R&D Program of China (2017YFA0604302), National Natural Science Foundation of China (41475099), and CAS Key Research Program of Frontier Sciences (QYZDY-SSW-DQC002). MVM is supported by the US Joint Fire Science Program (13-1-01-4) and the UK Leverhulme Trust through a Leverhulme Research Centre Award (RC-2015-029). AA acknowledges support from the Helmholtz Association, its ATMO programme and the Impulse and Networking fund which funded initial FireMIP activities. AA and SH acknowledge also the EU FP7 project BACCHUS (603445). BIM is supported by NSF (BCS-1436496). CI is supported by NASA (NNH12ZDA001N-IDS). We are grateful to Stéphane Mangeon for providing data of

JULES-INFERNO simulations, and R. J. Yokelson, Z.-D. Lin, S. Kloster, M. van Marle, B. Bond-Lamberty, and J. R. Marlon for helpful discussions.

Competing interests. The authors declare that they have no conflict of interest.

References

Akagi, S. K., Yokelson, R. J., Wiedinmyer, C., Alvarado, M. J., Reid, J. S., Karl, T., Crounse, J. D., and Wennberg, P. O.: Emission factors for open and domestic biomass burning for use in atmospheric models, Atmos. Chem. Phys., 11, 4039-4072, https://doi.org/10.5194/acp-11-4039-2011, 2011.

Andela, N., et al. : A human-driven decline in global burned area, Science, 356, 1356-1362, 2017.

Andela, N., Morton, D. C., Giglio, L., Paugam, R., Chen, Y., Hanson, S., van der Werf, G. R., and Randerson, J. T.: The Global Fire Atlas of individual fire size, duration, speed, and direction, Earth Syst. Sci. Data Dis., https://doi.org/10.5194/essd-2018-89, in review, 2018.

Andreae, M. O.: Emission of trace gases and aerosols from biomass burning – An update, Earth Syst. Sci. Data, in preparation.

Andreae, M. O. and Merlet, P.: Emission of trace gases and aerosols from biomass burning, Global Biogeochem. Cy., 15, 955–966, 2001.

Andreae, M. O. and Rosenfeld, D.: Aerosol–cloud– precipitation interactions, Part 1, The nature and sources of cloud-active aerosols, Earth-Sci. Rev., 89, 13–41, doi:10.1016/j.earscirev.2008.03.001, 2008.

Atmos. Chem. Phys. Discuss., https://doi.org/10.5194/acp-2019-37
Manuscript under review for journal Atmos. Chem. Phys.
Discussion started: 8 March 2019

Archibald, S.: Managing the human component of fire regimes: lessons from Africa, Philos. T. R. Soc. B., 371, 20150346, 2016.

Arora, V. K. and Boer, G.: Fire as an interactive component of dynamic vegetation models, J. Geophys. Res., 110, 2005.

Bachelet, K. Ferschweiler, T. J. Sheehan, B. M. Sleeter, and Z. Zhu: Projected carbon stocks in the conterminous USA with land use and variable fire regimes, Glob. Change Biol., 21, 4548–4560, 2015.

Best, M. J., et al.: The Joint UK Land Environment Simulator (JULES), model description – Part 1: Energy and water fluxes, Geosci. Model Dev., 4, 677–699, doi:10.5194/gmd-4-677-2011, http://www.geosci-model-dev.net/4/677/2011/, 2011.

Bistinas, S. P. Harrison, I. C. Prentice, and J. M. C. Pereira: Causal relationships versus emergent patterns in the global controls of fire frequency, Biogeosciences, 11, 5087–5101, 2014.

Bond-Lamberty, B., Peckham, S.D., Ahl, D.E., and Gower, S.T.:The dominance of fire in determining carbon balance of the central Canadian boreal forest, Nature, 450, 89–92, 2007.

Bowman, D. M. J. S., et al.: Fire in the Earth system, Science, 324, 481–484, 2009.

Brovkin, V.,et al.: Effect of anthropogenic land-use and land-cover changes on climate and land carbon storage in CMIP5 projections for the twenty-first century, J. Climate, 26, 6859–6881, doi:10.1175/JCLI-D-12-00623.1, http://journals.ametsoc.org/doi/abs/10.1175/JCLI-D-12-00623.1, 2013.

Atmos. Chem. Phys. Discuss., https://doi.org/10.5194/acp-2019-37
Manuscript under review for journal Atmos. Chem. Phys.
Discussion started: 8 March 2019

Chen, Y., Randerson, J., van der Werf, G., Morton, D., Mu, M., and Kasibhatla, P.: Nitrogen deposition in tropical forests from savanna and deforestation fires, Glob. Change Biol., 16, 2024–2038, 2010.

Ciais, P., C., et al.: Carbon and Other Biogeochemical Cycles, In: Climate Change 2013: The Physical Science Basis. Contribution of Working Group I to the Fifth Assessment Report of the Intergovernmental Panel on Climate Change, edited by: Stocker, T.F., Qin,D., Plattner, G.-K., Tignor, M., Allen, S.K., Boschung, J., Nauels, A., Xia, Y., Bex, V., and Midgley, P. M., Cambridge University Press, Cambridge, United Kingdom and New York, NY, USA, 467–544, 2013.

Clark, D. B. et al.: The Joint UK Land Environment Simulator (JULES), model description Part 2: Carbon fluxes and vegetation dynamics, Geosci. Model Dev., 4, 701–722, doi:10.5194/gmd-4-701-2011, http://www.geosci-model-dev.net/4/701/2011/, 2011.

Darmenov, A. S., and da Silva, A.: The Quick Fire Emissions Dataset (QFED): Documentation of versions 2.1, 2.2 and 2.4, In: Technical Report Series on Global Modeling and Data Assimilation, edited by Koster, R. D., NASA Goddard Space Flight Center; Greenbelt, MD, USA, pp. 212, 2015.

Duncan, B. N., Martin, R. V., Staudt, A. C., Yevich, R., and Logan, J. A.: Interannual and seasonal variability of biomass burning emissions constrained by satellite observations, J. Geophys. Res.-Atmos, 108, 4100, doi:10.1029/2002JD002378, 2003.

Ferretti, D. F., et al. : Unexpected changes to the global methane budget over the past

2000 years, Science, 309, 1714–1717, https://doi.org/10.1126/science.1115193, 2005.

Field, R. D., van der Werf, G. R., and Shen, S. S. P.: Human amplification of drought-induced biomass burning in Indonesia since 1960, Nat. Geosci., 2, 185–188, https://doi.org/10.1038/ngeo443, 2009.

Grandey, B. S., Lee, H.-H., and Wang, C.: Radiative effects of interannually varying vs. interannually invariant aerosol emissions from fires, Atmos. Chem. Phys., 16, 14495-14513, https://doi.org/10.5194/acp-16-14495-2016, 2016.

Hamilton, D. S., et al.: Reassessment of pre-industrial fire emissions strongly affects anthropogenic aerosol forcing, Nat. Commun., 9, 3182, doi: 10.1038/s41467-018-05592-9, 2018.

Hantson, S., Pueyo, S., and Chuvieco, E.: Global fire size distribution is driven by human impact and climate, Global Ecol. Biogeogr., 24, 77–86, 2015.

Hantson, S., et al.: The status and challenge of global fire modelling, Biogeosciences, 13, 3359–3375, doi:10.5194/bg-13-3359-2016, 2016.

Heymann, J., Reuter, M., Buchwitz, M., Schneising, O., Bovensmann, H., Burrows, J. P., Massart, S., Kaiser, J. W., and Crisp, D.: CO_2 emission of Indonesian fires in 2015 estimated from satellite-derived atmospheric CO_2 concentrations, Geophys. Res. Lett., 44, 1537–1544, 2017.

Hurtt, G. C., et al.: Harmonization of land-use scenarios for the period 1500–2100: 600 years of global gridded annual land-use transitions, wood harvest, and resulting secondary lands, Climatic Change, 109, 117–161, doi:10.1007/s10584-011-0153-2, 2011.

Ichoku, C. and Ellison, L.: Global top-down smoke-aerosol emissions estimation using satellite fire radiative power measurements, Atmos. Chem. Phys., 14, 6643-6667, https://doi.org/10.5194/acp-14-6643-2014, 2014.

Jiang, Y., Lu, Z., Liu, X. Qian, Y., Zhang, K., Wang, Y., and Yang, X.: Impacts of global wildfire aerosols on direct radiative, cloud and surface-albedo forcings simulated with CAM5, Atmos. Chem. Phys., 16, 14805-14824, 2016

Johnston, F. H., et al.: Estimated global mortality attributable to smoke from landscape fires, Environ. Health Persp., 120, 695–701. https://doi.org/10.1289/ehp.1104422, 2012.

Kaiser, J. W., Heil, A., Andreae, M. O., Benedetti, A., Chubarova, N., Jones, L., Morcrette, J.-J., Razinger, M., Schultz, M. G., Suttie, M., and van der Werf, G. R.: Biomass burning emissions estimated with a global fire assimilation system based on observed fire radiative power, Biogeosciences, 9, 527–554, https://doi.org/10.5194/bg-9-527-2012, 2012.

Keenan, T. F., Hollinger, D. Y., Bohrer, G., Dragoni, D., Munger, J. W., Schmid, H. P., and Richardson, A. D.: Increase in forest water-use efficiency as atmospheric carbon dioxide concentrations rise, Nature, 499, 324–327, 2013.

Klein Goldewijk, K., Beusen, A., and Janssen, P.: Long-term dynamic modeling of global population and built-up area in a spatially explicit way: HYDE 3.1, Holocene, 20, 565–573, https://doi.org/10.1177/0959683609356587, 2010.

Atmos. Chem. Phys. Discuss., https://doi.org/10.5194/acp-2019-37
Manuscript under review for journal Atmos. Chem. Phys.
Discussion started: 8 March 2019

Kloster, S., and Lasslop, G.: Historical and future fire occurrence (1850 to 2100) simulated in CMIP5 Earth System Models, Global Planet. Change, 58-69, 2017.

Kloster, S., Mahowald, N. M., Randerson, J. T., Thornton, P. E., Hoffman, F. M., Levis, S., Lawrence, D. M.: Fire dynamics during the 20th century simulated by the Community Land Model. Biogeosciences, 7(6), 1877–1902. https://doi.org/10.5194/bg-7-1877-2010, 2010.

Knorr, W., Dentener, F., Lamarque, J.-F., Jiang, L., and Arneth, A.: Wildfire air pollution hazard during the 21st century, Atmos. Chem. Phys., 17, 9223-9236, https://doi.org/10.5194/acp-17-9223-2017, 2017.

Knorr,W., Jiang, L., and Arneth, A.: Climate, CO2 and human population impacts on global wildfire emissions, Biogeosciences, 13, 267–282, https://doi.org/10.5194/bg-13-267-2016, 2016.

Kondo, M., et al.: Land use change and El Niño-Southern Oscillation drive decadal carbon balance shifts in Southeast Asia, Nat. Commun., 9, 1154, doi: 10.1038/s41467-018-03374-x, 2018.

Konovalov, I. B., Berezin, E. V., Ciais, P., Broquet, G., Beekmann, M., Hadji- Lazaro, J., Clerbaux, C., Andreae, M. O., Kaiser, J. W., and Schulze, E.: Constraining CO2 emissions from open biomass burning by satellite observations of co-emitted species: a method and its application to wildfires in Siberia, Atmos. Chem. Phys., 14, 10383–10410, 2014.

Krinner, G., Viovy, N., de Noblet-Ducoudré, N., Ogée, J., Polcher, J., Friedlingstein, P., Ciais, P., Sitch, S., and Prentice, I. C.: A dynamic global vegetation model for

Atmos. Chem. Phys. Discuss., https://doi.org/10.5194/acp-2019-37
Manuscript under review for journal Atmos. Chem. Phys.
Discussion started: 8 March 2019

studies of the coupled atmosphere-biosphere system, Global Biogeochem. Cy., 19, 1–33, https://doi.org/10.1029/2003GB002199, 2005.

Krol, M., Peters, W., Hooghiemstra, P., George, M., Clerbaux, C., Hurtmans, D., McInerney, D., Sedano, F., Bergamaschi, P., El Hajj, M., Kaiser, J. W., Fisher, D., Yershov, V., and Muller, J.-P.: How much CO was emitted by the 2010 fires around Moscow? Atmos. Chem. Phys., 13(9):4737–4747, 2013.

Lamarque, J.-F., et al.: Historical (1850–2000) gridded anthropogenic and biomass burning emissions of reactive gases and aerosols: methodology and application, Atmos. Chem. Phys., 10, 7017-7039, https://doi.org/10.5194/acp-10-7017-2010, 2010.

Lasslop, G., Thonicke, K., and Kloster, S.: SPITFIRE within the MPI Earth system model: Model development and evaluation, J. Adv. Model Earth Sy., 6, 740–755, https://doi.org/10.1002/2013MS000284, 2014.

Legrand, M., et al.: Boreal fire records in Northern Hemisphere ice cores: a review, Clim. Past, 12, 2033-2059, https://doi.org/10.5194/cp-12-2033-2016, 2016.

Lehsten, V., Tansey, K., Balzter, H., Thonicke, K., Spessa, A., Weber, U., Smith, B., and Arneth, A.: Estimating carbon emissions from African wildfires, Biogeosciences, 6, 349-360, https://doi.org/10.5194/bg-6-349-2009, 2009.

Lelieveld, J., Evans, J. S., Fnais, M., Giannadaki, D., and Pozzer, A.: The contribution of outdoor air pollution sources to premature mortality on a global scale, Nature, 525, 367– 371, 2015.

Le Page, Y., Morton, D., Bond-Lamberty, B., Pereira, J. M. C., and Hurtt, G.: HESFIRE: A global fire model to explore the role of anthropogenic and weather drivers, Biogeosciences, 12, 887–903, https://doi.org/10.5194/bg-12-887-2015, 2015.

Le Quéré, C.,et al.: Global carbon budget 2013, Earth Syst. Sci. Data, 6, 235–263, doi:10.5194/essd-6-235-2014, http://www.earth-syst-sci-data.net/6/235/2014/, 2014.

Levis, S., Bonan, G. B., Vertenstein, M., and Oleson, K. W.: The Community Land Model's dynamic global vegetation model (CLM-DGVM): Technical description and user's guide, NCAR Tech. Note TN-459 IA, Terrestrial Sciences Section, Boulder, Colorado, 2004

Li, F., Zeng, X.-D., Levis, S.: A process-based fire parameterization of intermediate complexity in a Dynamic Global Vegetation Model, Biogeosciences, 9, 2761–2780, 2012.

Li, F., Levis, S., and Ward, D.S.: Quantifying the role of fire in the Earth system–Part 1: Improved global fire modeling in the Community Earth System Model (CESM1), Biogeosciences, 10, 2293–2314, 2013.

Li, F., and Lawrence, D.M.: Role of fire in the global land water budget during the 20th century through changing ecosystems, J. Clim., 30, 1893–908, 2017.

Li, F., Lawrence, D.M., Bond-Lamberty, B.: Human impacts on 20th century fire dynamics and implications for global carbon and water trajectories, Glob. Planet. Change, 162, 18-27, 2018.

Atmos. Chem. Phys. Discuss., https://doi.org/10.5194/acp-2019-37
Manuscript under review for journal Atmos. Chem. Phys.
Discussion started: 8 March 2019

Lindeskog, M., Arneth, A., Bondeau, A.,Waha, K., Seaquist, J., Olin, S., and Smith, B.: Implications of accounting for land use in simulations of ecosystem carbon cycling in Africa, Earth Syst. Dynam,, 4, 385–407, doi:10.5194/esd-4-385-2013, 2013.

Magi, B.I., Rabin, S., Shevliakova, E., Pacala, S.: Separating agricultural and non-agricultural fire seasonality at regional scales, Biogeosciences, 9, 3003–3012, 2012.

Mahowald, N., et al.: Global distribution of atmospheric phosphorus sources, concentrations and deposition rates, and anthropogenic impacts, Global Biogeochem. Cy., 22, GB4026, doi: 10.1029/2008GB003240, 2008.

Mangeon, S., Voulgarakis, A., Gilham, R., Harper, A., Sitch, S., and Folberth, G.: INFERNO: a fire and emissions scheme for the UK Met Office's Unified Model, Geosci. Model Dev., 9, 2685–2700, doi:10.5194/gmd-9-2685-2016, http://www.geosci-model-dev.net/9/2685/2016/, 2016.

Mao, J. F., Wang, B., and Dai, Y. J.: Sensitivity of the carbon storage of potential vegetation to historical climate variability and CO_2 in continental China, Adv. Atmos. Sci., 26, 87–100, 2009.

Marlier, M. E., DeFries, R. S., Voulgarakis, A., Kinney, P. L., Randerson, J. T., Shindell, D. T., Chen, Y., and Faluvegi, G.: El Niño and health risks from landscape fire emissions in southeast Asia, Nat. Clim. Change, 3, 131–136, 2013.

Marlon, J. R., et al.: Climate and human influences on global biomass burning over the past two millennia, Nat. Geosci., 1, 697–702,

Atmos. Chem. Phys. Discuss., https://doi.org/10.5194/acp-2019-37
Manuscript under review for journal Atmos. Chem. Phys.
Discussion started: 8 March 2019

Atmospheric Chemistry and Physics Discussions
Open Access

https://doi.org/10.1038/ngeo313, 2008.

Marlon, J. R., et al.: Reconstructions of biomass burning from sediment–charcoal records to improve data–model comparisons, Biogeosciences, 13, 3225–3244, https://doi.org/10.5194/bg-13-3225-2016, 2016.

McKendry, I. G., Christen, A., Lee, S.-C., Ferrara, M., Strawbridge, K. B., O'Neill, N., and Black, A.: Impacts of an Intense Wildfire Smoke Episode on Surface Radiation, Energy and Carbon Fluxes in Southwestern British Columbia, Canada, Atmos. Chem. Phys. Dis., https://doi.org/10.5194/acp-2018-252, in review, 2018.

McMeeking, G. R., et al.: Emissions of trace gases and aerosols during the open combustion of biomass in the laboratory, J. Geophys. Res.,114, D19210, doi:10.1029/2009JD011836, 2009.

Melton, J. R., and Arora, V. K.: Competition between plant functional types in the Canadian Terrestrial Ecosystem Model (CTEM) v. 2.0, Geosci. Model Dev., 9, 323–361, doi:10.5194/gmd-9-323-2016, 2016.

Mieville, A., Granier, C., Liousse, C., Guillaume, B., Mouillot, F., Lamarque, J.-F., Grégoire, J.-M., and Pétron, G.: Emissions of gases and particles from biomass burning during the 20th century using satellite data and an historical reconstruction, Atmos. Environ., 44, 1469–1477, https://doi.org/10.1016/j.atmosenv.2010.01.011, 2010.

Atmos. Chem. Phys. Discuss., https://doi.org/10.5194/acp-2019-37
Manuscript under review for journal Atmos. Chem. Phys.
Discussion started: 8 March 2019

Mouillot, F. and Field, C. B.: Fire history and the global carbon budget: a $1^{o}\times1^{o}$fire history reconstruction for the 20th century, Glob. Change Biol., 11, 398–420, https://doi.org/10.1111/j.1365-2486.2005.00920.x, 2005.

Nemani, R.R., and Running, S.W.: Implementation of a hierarchical global vegetation classification in ecosystem function models, J. Veg. Sci., 7, 337-346, 1996.

Oleson, K., et al..: Technical Description of version 4.5 of the Community Land Model (CLM), Tech. Rep. NCAR/TN-503+STR NCAR, Boulder, CO, USA, pp.434, 2013.

Parisien, M., Miller, C., Parks, S.A., DeLancey, E.R., Robinne, F., and Flannigan, M. D.: The spatially varying influence of humans on fire probability in North America, Environ. Res. Lett., 11:075005, 2016.

Pechony, O., and Shindell, D.T.: Driving forces of global wildfires over the past millennium and the forthcoming century, P. Natl. Acad. Sci. USA, 107, 19167–19170, 2010.

Pfeiffer, M., Spessa, A., and Kaplan, J. O.: A model for global biomass burning in preindustrial time: LPJ-LMfire (v1.0), Geosci. Model Dev., 6, 643–685, doi:10.5194/gmd-6-643-2013, 2013.

Rabin, S. S., et al.: The Fire Modeling Intercomparison Project (FireMIP), phase 1: experimental and analytical protocols with detailed model descriptions. Geosci. Model Dev., 10, 1175-1197, 2017.

Rabin, S. S., Ward, D. S., Malyshev, S. L., Magi, B. I., Shevliakova, E., and Pacala, S. W.: A fire model with distinct crop, pasture, and non-agricultural burning: use of new data and a model-fitting algorithm for FINAL.1, Geosci. Model Dev., 11, 815-842, https://doi.org/10.5194/gmd-11-815-2018, 2018.

Rothermel, R. C.:A mathematical model for predicting fire spread in wildland fuels, Res. Pap. INT-115, US Department of Agriculture, Ogden, UT, USA, pp. 40, 1972.

Schultz, M. G., Heil, A., Hoelzemann, J. J., Spessa, A., Thonicke, K., Goldammer, J. G., Held, A. C., Pereira, J. M. C., and van het Bolscher, M.: Global wildland fire emissions from 1960 to 2000, Global Biogeochem. Cy., 22, GB2002, https://doi.org/10.1029/2007GB003031, 2008.

Scott, A. C., and Glasspool, I. J.: The diversification of Palaeozoic fire systems and fluctuations in atmospheric oxygen concentration, Proc. Natl. Acad. Sci. U.S.A., 103, 10861–10865, doi:10.1073/pnas.0604090103, 2006.

Sheehan, T., Bachelet, D., and Ferschweiler, K.: Projected major fire and vegetation changes in the Pacific Northwest of the conterminous United States under selected CMIP5 climate futures, Ecol. Model., 317, 16–29, doi:10.1016/j.ecolmodel.2015.08.023, 2015.

Smith, B., Wårlind, D., Arneth, A., Hickler, T., Leadley, P., Siltberg, J., and Zaehle, S.: Implications of incorporating N cycling and N limitations on primary production in an individual-based dynamic vegetation model, Biogeosciences, 11, 2027–2054, doi:10.5194/bg-11-2027-2014, 2014.

Stockwell, C. E., et al.: Nepal Ambient Monitoring and Source Testing Experiment (NAMaSTE): emissions of trace gases and light-absorbing carbon from wood and dung cooking fires, garbage and crop residue burning, brick kilns, and other sources, Atmos. Chem. Phys., 16, 11043-11081, 2016.

Thonicke, K., Spessa, A., Prentice, I. C., Harrison, S. P., Dong, L., and Carmona-Moreno, C.: The influence of vegetation, fire spread and fire behaviour on biomass burning and trace gas emissions: Results from a process-based model, Biogeosciences, 7, 1991–2011, 2010.

Thonicke, K., Venevsky, S., Sitch, S., and Cramer, W.: The role of fire disturbance for global vegetation dynamics: Coupling fire into a Dynamic Global Vegetation Model, Global Ecol. Biogeogr., 10, 661–677, 2001.

Thornhill, G. D., Ryder, C. L., Highwood, E. J., Shaffrey, L. C., and Johnson, B. T.: The effect of South American biomass burning aerosol emissions on the regional climate, Atmos. Chem. Phys., 18, 5321-5342, https://doi.org/10.5194/acp-18-5321-2018, 2018.

Tian, H., et al.: The terrestrial biosphere as a net source of greenhouse gases to the atmosphere, Nature, 531, 225–228, 2016.

Tosca, M. G., Randerson, J. T., and Zender, C. S.: Global impact of smoke aerosols from landscape fires on climate and the Hadley circulation, Atmos. Chem. Phys., 13, 5227–5241, https://doi.org/10.5194/acp-13-5227-2013, 2013

Val Martin, M., Heald, C.L., Lamarque, J.F., Tilmes, S., Emmons, L.K., Schichtel, B.A.: How emissions, climate, and land use change will impact mid-century air quality over the United States: a focus on effects at national parks, Atmos. Chem. Phys. 15, 2805-2823, 2015.

Atmos. Chem. Phys. Discuss., https://doi.org/10.5194/acp-2019-37
Manuscript under review for journal Atmos. Chem. Phys.
Discussion started: 8 March 2019

van der Werf, G. R., Peters, W., van Leeuwen, T. T., and Giglio, L: What could have caused pre-industrial biomass burning emissions to exceed current rates?, Clim. Past, 9, 289–306, http://www.clim-past.net/9/289/2013/, 2013.

van der Werf, G. R., Randerson, J. T., Giglio, L., Collatz, G. J., Mu, M., Kasibhatla, P. S., Morton, D. C., DeFries, R. S., Jin, Y., and van Leeuwen, T. T.: Global fire emissions and the contribution of deforestation, savanna, forest, agricultural, and peat fires (1997–2009), Atmos. Chem. Phys., 10, 11707–11735, https://doi.org/10.5194/acp-10-11707-2010, 2010.

van der Werf, G. R., et al.: Global fire emissions estimates during 1997–2016, Earth Syst. Sci. Data., 9, 679-720, 2017.

van Marle, M. J. E., Field, R. D., van der Werf, G. R., Estrada de Wagt, I. A., Houghton, R. A., Rizzo, L. V., Artaxo, P., and Tsigaridis, K.: Fire and deforestation dynamics in Amazonia (1973–2014), Global Biogeochem. Cy., 31, 24–38,https://doi.org/10.1002/2016GB005445, 2017a.

van Marle, M. J. E., et al., Historic global biomass burning emissions based on merging satellite observations with proxies and fire models (1750 - 2015), Geosci. Model Dev. , 10, 3329-3357, doi:10.5194/gmd-2017-32, 2017b.

Wang, Z., et al.: The isotopic record of Northern Hemisphere atmospheric carbon monoxide since 1950: implications for the CO budget, Atmos. Chem. Phys., 12, 4365–4377, https://doi.org/10.5194/acp-12-4365-2012, 2012.

Ward, D. S., Kloster, S., Mahowald, N. M., Rogers, B.M., Randerson, J. T., Hess, P. G.: The changing radiative forcing of fires: Global model estimates for past, present and future, Atmos. Chem. Phys. 12, 10857–10886, 2012.

Ward, D. S., Shevliakova, E., Malyshev, S., Rabin, S.: Trends and variability of global fire emissions due to historical anthropogenic activities. Global Biogeochem. Cy.,32, 122–142, https://doi.org/10.1002/2017GB005787, 2018.

Wei, Y., et al.: The North American Carbon Program Multi-scale Synthesis and Terrestrial Model Intercomparison Project – Part 2: Environmental driver data, Geoscientific Model Development, 7, 2875–2893, doi:10.5194/gmd-7-2875-2014, 2014.

Wiedinmyer, C., Akagi, S. K., Yokelson, R. J., Emmons, L. K., Al-Saadi, J. A., Orlando, J. J., and Soja, A. J. : The Fire INventory from NCAR (FINN): A high resolution global model to estimate the emissions from open burning, Geosci. Model Dev., 4, 625–641, https://doi.org/10.5194/gmd-4-625-2011, 2011

Wu, Y., Han, Y., Voulgarakis, A., Wang, T., Li, M., Wang, Y., Xie, M., Zhuang, B., and Li, S.: An agricultural biomass burning episode in eastern China: Transport, optical properties, and impacts on regional air quality, J. Geophys. Res.-Atmos., 122, 2304–2324, doi:10.1002/2016JD025319, 2017.

Yang, J., Tian, H., Tao, B., Ren, W., Kush, J., Liu, Y., and Wang, Y.: Spatial and temporal patterns of global burned area in response to anthropogenic and environmental factors: Reconstructing global fire history for the 20th and early

Atmos. Chem. Phys. Discuss., https://doi.org/10.5194/acp-2019-37
Manuscript under review for journal Atmos. Chem. Phys.
Discussion started: 8 March 2019

21st centuries, J. Geophys. Res, -Biogeo., 119, 249–263. https://doi.org/10.1002/2013JG002532, 2014.

Yokelson, R. J., et al.: Coupling field and laboratory measurements to estimate the emission factors of identified and unidentified trace gases for prescribed fires, Atmos. Chem. Phys., 13, 89–116, doi:10.5194/acp-13-89-2013, 2013.

Yue, C., Ciais, P., Cadule, P., Thonicke, K., and van Leeuwen, T. T.: Modelling the role of fires in the terrestrial carbon balance by incorporating SPITFIRE into the global vegetation model ORCHIDEE– Part 2: Carbon emissions and the role of fires in the global carbon balance, Geosci. Model Dev., 8, 1321–1338, https://doi.org/10.5194/gmd-8-1321-2015, 2015.

Yue, C., et al.: Modelling the role of fires in the terrestrial carbon balance by incorporating SPITFIRE into the global vegetation model ORCHIDEE – Part 1: simulating historical global burned area and fire regimes, Geosci. Model Dev., 7, 2747–2767, https://doi.org/10.5194/gmd-7-2747-2014, 2014.

Yue, X., and Unger, N. : Fire air pollution reduces global terrestrial productivity, nature commun., 9, 5413, https://doi.org/10.1038/s41467-018-07921-4, 2018.

Zennaro, P., et al.: Fire in ice: two millennia of boreal forest fire history from the Greenland NEEM ice core, Clim. Past, 10, 1905–1924, https://doi.org/10.5194/cp-10-1905-2014, 2014.

Zhang, F., Wang, J., Ichoku, C., Hyer, E. J., Yang, Z., Ge, C., Su, S., Zhang, X., Kondragunta, S., Kaiser, J. W., Wiedinmyer, C., and da Silva, A.: Sensitivity of mesoscale modeling of smoke direct radiative effect to the emission inventory: a case study in northern sub-Saharan African region, Environ. Res. Lett., 9, 075002, doi:10.1088/1748-9326/9/7/075002, 2014.

Zhu, Z., et al: Greening of the Earth and its drivers, Nat. Clim. Change, 6, 791–795, 2016.

Atmos. Chem. Phys. Discuss., https://doi.org/10.5194/acp-2019-37
Manuscript under review for journal Atmos. Chem. Phys.
Discussion started: 8 March 2019

Atmospheric Chemistry and Physics Discussions
Open Access

Table 1. Summary description of the Dynamic Global Vegetation Models (DGVMs) participated in FireMIP.

DGVMs	tem. res. of model outputs	spatial res. of model outputs	period	natural veg. distrib.	specific treat for pastures	crop fires	tropical human defor. fires	human ignition	human suppression on fires	peat fires	fire scheme ref.	DGVM ref.
CLM4.5 but CLM5 fire model (CLM4.5)	monthly	~1.9° (lat) ×2.5° (lon)	1700–2012	P	no pasture PFTs	yes	yes	increase with PD	occurrence & spread area[a]	yes[d]	Li et al. (2012, 2013) Li and Lawrence (2017)	Oleson et al. (2013)
CTEM	monthly	2.8125°	1861–2012	P	no pasture PFTs	no	no	increase with PD	occurrence & duration[b]	no	Arora and Boer (2005) Melton and Arora 2016	Melton and Arora (2016)
JSBACH-SPITFIRE (JSBACH)	monthly	1.875°	1700–2012	P	high fuel bulk dens.	no	no	increase with PD	occurrence & duration[b]	no	Lasslop et al. (2014) Thonicke et al. (2010)	Brovkin et al. (2013)
JULES-INFERNO (JULES)	monthly	~1.2° (lat) ×1.9°(lon)	1700–2012	M	no pasture PFTs	no crop PFTs	no	increase with PD	occurrence[b]	no	Mangeon et al. (2016)	Best et al. (2011) Clark et al. (2011)
LPJ-GUESS-GlobFIRM (LGG)	annual	0.5°	1700–2012	M	harvest	no	no	no	no	no	Thonicke et al. (2001)	Smith et al. (2014) Lindeskog et al. (2013)
LPJ-GUESS-SPITFIRE (LGS)	monthly	0.5°	1700–2012	M	no pasture PFTs	no crop PFTs	no	increase with PD	occurrence[b]	no	Lehsten et al. (2009) Rabin et al. (2017)	Smith et al. (2001) Ahlstrom et al. (2012)
LPJ-GUESS-SIMFIRE -BLAZE (LGSB)	monthly	0.5°	1700–2012	M	harvest	no	no	increase with PD	burned area[b]	no	Knorr et al. (2016)	Smith et al. (2014) Lindeskog et al. (2013) Nieradzik et al. (2017)
MC2	annual	0.5°	1901–2008	M	no pasture PFTs	no crop PFTs	no	no	occurrence[c]	no	Bachelet et al. (2015) Sheehan et al. (2015)	Bachelet et al. (2015) Sheehan et al. (2015)
ORCHIDEE-SPITFIRE (ORCHIDEE)	monthly	0.5°	1700–2012	P	no pasture PFTs	no	no	increase with PD	occurrence[b]	no	Yue et al. (2014, 2015) Thonicke et al. (2010)	Krinner et al. (2005)

Acronym: CLM4.5 and CLM5: Community Land Model version 4.5 and 5; CTEM: Canadian Terrestrial Ecosystem Model; JSBACH: Jena Scheme for Biosphere-Atmosphere Coupling in Hamburg; SPITFIRE: Spread and InTensity fire model;

Atmos. Chem. Phys. Discuss., https://doi.org/10.5194/acp-2019-37
Manuscript under review for journal Atmos. Chem. Phys.
Discussion started: 8 March 2019

JULES: Joint UK Land Environment Simulator; INFERNO: Interactive Fire And Emission Algorithm For Natural Environments; GlobFIRM: fire module Global FIRe Model; SMIFIRE: SIMple FIRE model; BLAZE: Blaze-Induced Land-Atmosphere Flux Estimator; ORCHIDEE: Organizing Carbon Hydrology In Dynamic Ecosystems;

PFT: plant functional type; P: prescribed; M: modeled; PD: population density

[a] fire suppression increases with PD and GDP, different between tree PFTs and grass/shrub PFTs

[b] fire suppression increases with PD

[c] Assume no fire in grid cell when pre-calculated rate of spread, fireline intensity, and energy release component are lower than thresholds

[d] CLM4.5 outputs in FireMIP include biomass and litter burning due to peat fires, but don't include burning of soil organic matter

Atmos. Chem. Phys. Discuss., https://doi.org/10.5194/acp-2019-37
Manuscript under review for journal Atmos. Chem. Phys.
Discussion started: 8 March 2019

Atmospheric Chemistry and Physics Discussions
Open Access
EGU

Table 2. Emission factors (g specie (kg DM)$^{-1}$) for land cover types (LCTs).

No.	Species	grassland /savanna	tropical forest	temperate forest	boreal forest	cropland
1	CO_2	1647	1613	1566	1549	1421
2	CO	70	108	112	124	78
3	CH_4	2.5	6.3	5.8	5.1	5.9
4	NMHC	5.5	7.1	14.6	5.3	5.8
5	H2	0.97	3.11	2.09	1.66	2.65
6	NO_x	2.58	2.55	2.90	1.69	2.67
7	N_2O	0.18	0.20	0.25	0.25	0.09
8	$PM_{2.5}$	7.5	8.3	18.1	20.2	8.5
9	TPM	8.5	10.9	18.1	15.3	11.3
10	TPC	3.4	6.0	8.4	10.6	5.5
11	OC	3.1	4.5	8.9	10.1	5.0
12	BC	0.51	0.49	0.66	0.50	0.43
13	SO_2	0.51	0.78	0.75	0.75	0.81
14	C_2H_6 (ethane)	0.42	0.94	0.71	0.90	0.76
15	CH_3OH (methanol)	1.48	3.15	2.13	1.53	2.63
16	C_3H_8 (propane)	0.14	0.53	0.29	0.28	0.20
17	C_2H_2 (acetylene)	0.34	0.43	0.35	0.27	0.32
18	C_2H_4 (ethylene)	1.01	1.11	1.22	1.49	1.14
19	C_3H_6 (propylene)	0.49	0.86	0.67	0.66	0.48
20	C_5H_8 (isoprene)	0.12	0.22	0.19	0.07	0.18
21	$C_{10}H_{16}$ (terpenes)	0.10	0.15	1.07	1.53	0.03
22	C_7H_8 (toluene)	0.20	0.23	0.43	0.32	0.18
23	C_6H_6 (benzene)	0.34	0.38	0.46	0.52	0.31
24	C_8H_{10} (xylene)	0.09	0.09	0.17	0.10	0.09
25	CH_2O (formaldehyde)	1.33	2.40	2.22	1.76	1.80
26	C_2H_4O (acetaldehyde)	0.86	2.26	1.20	0.78	1.82
27	C_3H_6O (acetone)	0.47	0.63	0.70	0.61	0.61
28	$C_3H_6O_2$(hydroxyacetone)	0.52	1.13	0.85	1.48	1.74
29	C_6H_5OH (Phenol)	0.37	0.23	0.33	2.96	0.50
30	NH_3 (ammonia)	0.91	1.45	1.00	2.82	1.04
31	HCN (hydrogen cyanide)	0.42	0.38	0.62	0.81	0.43
32	MEK/2-butanone	0.13	0.50	0.23	0.15	0.60
33	CH_3CN (acetonitrile)	0.17	0.51	0.23	0.30	0.25

Atmos. Chem. Phys. Discuss., https://doi.org/10.5194/acp-2019-37
Manuscript under review for journal Atmos. Chem. Phys.
Discussion started: 8 March 2019

Table 3. Attribution of plant function types (PFTs) in FireMIP DGVMs to land cover types (LCTs) for emission factors described in Table 2.

LCT / Models	Grassland /Savannas	Tropical Forest	Temperate Forest	Boreal Forest	Cropland
CLM4.5	A C3/C3/C4 G	Tro BE T	Tem NE T	Bor NE T	Crop
	Bor BD S	Tro BD T	Tem BE T	Bor ND T	
	Tem BE/BD S		Tem BD T	Bor BD T	
CTEM	C3/C4 G	BE T[a]	NE/BE T[a]	NET[a], ND T	C3/C4 Crop
		Other BD T[a]	Other BD T[a]	Cold BD T	
JSBACH	C3/C4 G/P	Tro E/D T	Ex-Tro E/D T[a]	Ex-Tro E/D T[a]	Crop
JULES	C3/C4 G	Tro BE T	Tem BE T	BD/NE T[a]	
	E/D S	BD T[a]	BD/NE T[a]	NDT	
LGG[b]	C3/C4 G	Tro BE/BR T	Tem NSG/BSG/BE T	Bor NE T	R/I S/W Wheat
	C3/C4 G in P	Tro SI BE T	Tem SI SG B T	Bor SI NE T	R/I Maize
LGS	C3/C4 G	Tro BE/BR T	Tem SI/&SG B T	Bor NE T	
		Tro SI BE T	Tem B/N E T	Bor SI/&SG NE/N T	
LGSB[b]	C3/C4 G	Tro BE/BR T	Tem NSG/BSG/ BE T	Bor NE T	R/I S/W Wheat
	C3/C4 G in P	Tro SI BE T	Tem SI SG B T	Bor SI NE T	R/I Maize
MC2	Tem C3 G/S	Tro BE T	Maritime NE F	Bor NE F	
	Sub-Tro C4 G/S	Tro D W[c]	Sub-Tro NE/BD/BE/M F	Subalpine F	
	Tro S/G/Sava			Cool N F	
	Bor M W		Tem NE/BD F		
	Tem/Sub-Tro NE/B/M W		Tem C/W M F		
	Tundra				
	Taiga-Tundra				
ORCHIDEE	C3/C4 G	Tro B E/R T	Tem N/B E T	Bor N E/D T	C3/C4 Crop
			Tem BD T	Bor BT T	

Acronym: T: tree; S: shrub; W: woodland; F: forest; G: grass; P: pasture; Sava: Savanna; N: needleleaf; E: evergreen; B: broadleaf; D: deciduous; R: raingreen; SI: shaded-intolerant; SG: summer-green; M: mixed; I: irrigated; RF: rainfed; C/W: cool or warm; S/W: spring or winter, Tro: Tropical; Tem: Temperate; Bor: Boreal; Sub-Tro: subtropical; Ex-Tro: Extratropical; A: Arctic

[a] split tree PFTs into tropical, temperate, and boreal groups following rules of Nemani and Running (1996) that also used to make CLM land surface data by Peter et al. (2007; 2012) since CLM version 3

[b] LGG and LGBS did not outputs PFT-level fire carbon emissions, so land cover classified using its dominant vegetation type

[c] MC2 classifies tropical savannas and tropical deciduous woodland regions, and the latter mainly represents tropical deciduous forests

Atmos. Chem. Phys. Discuss., https://doi.org/10.5194/acp-2019-37
Manuscript under review for journal Atmos. Chem. Phys.
Discussion started: 8 March 2019

Table 4. Summary description of satellite-based products and historical constructions merged from multiple sources.

Name	Method	Fire data sources	Peat burning	Start year	reference
GFED4	Bottom-up: fuel consumption,	MODIS,VIRS/ATSR	Y	1997	van der Werf et al. (2017)
GFED4s	burned area &active fire counts		Y	1997	
GFAS1.2	(GFED4&4s), FRP (GFAS1),	MODIS	Y	2001	Kaiser et al. (2012)
FINN1.5	active fire counts (FINN1.5), emis. factor	MODIS	N	2003	Wiedinmyer et al. (2011)
FEER1	Top-down: FRP, satellite AOD	MODIS, SEVIRI	Y	2003	Ichoku and Ellison (2014)
QFED2.5	constrained, emis. factor	MODIS	N	2001	Darmenov and da Silva (2015)
CMIP5	Merged decadal fire trace gas and aerosol emis.	GFED2, GICC, RETRO (model GlobFIRM used)	Y	1850	Lamarque et al. (2010)
CMIP6	Merged monthly fire carbon emis., present-day veg. dist., emis. factor	GFED4s, FireMIP models, GCDv3 charcoal records, WMO visibility obs.	Y	1750	van Marle et al. (2017)

Acronym: GFED4: Global Fire Emissions Dataset version 4; GFED4s: GFED4 with small fires; GFAS1.2: Global Fire Assimilation System version 1.2; FINN1.5: Fire Inventory from NCAR version 1.5; FRP: fire radiative power; FEER1: Fire emissions from the Fire Energetics and Emissions Research version1; QFED2.5: Quick Fire Emissions Dataset version 2.5; AOD: aerosol optical depth; GFED2: GFED version 2; RETRO: REanalysis of the TROpospheric chemical composition; GICC: Global Inventory for Chemistry-Climate studies; GCDv3: Global Charcoal Database version 3

Table 5. Global total of fire emissions from 2003 to 2008 for DGVMs in FireMIP and benchmarks. Unit: Pg (Pg=10^{15}g)

Source	C	CO_2	CO	CH_4	BC	OC	$PM_{2.5}$
FireMIP							
CLM4.5	2.1	6.5	0.36	0.018	0.0021	0.020	0.042
CTEM	3.0	8.9	0.48	0.025	0.0028	0.030	0.060
JSBACH	2.1	6.5	0.32	0.013	0.0020	0.016	0.036
JULES	2.1	6.9	0.44	0.024	0.0022	0.020	0.039
LGG	4.9	15.4	0.90	0.047	0.0050	0.048	0.097
LGS	1.7	5.6	0.26	0.011	0.0017	0.012	0.027
LGSB	2.5	7.7	0.48	0.025	0.0025	0.024	0.047
MC2	1.0	3.1	0.18	0.008	0.0011	0.012	0.025
ORCHIDEE	2.8	9.2	0.44	0.018	0.0029	0.020	0.045
Benchmarks							
GFED4	1.5	5.4	0.24	0.011	0.0013	0.012	0.025
GFED4s	2.2	7.3	0.35	0.015	0.0019	0.016	0.036
GFAS1.2	2.1	7.0	0.36	0.019	0.0021	0.019	0.030
FINN1.5	2.0	7.0	0.36	0.017	0.0021	0.022	0.039
FEER1	4.2	14.0	0.65	0.032	0.0042	0.032	0.054
QFED2.5	----	8.2	0.39	0.017	0.0060	0.055	0.086

Atmos. Chem. Phys. Discuss., https://doi.org/10.5194/acp-2019-37
Manuscript under review for journal Atmos. Chem. Phys.
Discussion started: 8 March 2019

Table 6. Temporal correlation of annual global fire $PM_{2.5}$ emissions between FireMIP models and satellite-based GFED4 and GFED4s (1997–2012), GFAS1.2 and QFED2.5 (2001–2012), and FINN1.5 and FEER1 (2003–2012).

DGVMs	GFED4	GFED4s	GFAS1.2	FINN1.5	FEER1	QFED2.5
CLM4.5	0.73***	0.79***	0.63**	0.62*	0.55*	0.58**
CTEM	0.51**	0.54**	0.63**	0.60*	0.52	0.68**
JSBACH	–0.18	–0.42	0.10	0.02	–0.04	0.32
JULES	0.33	0.31	0.31	0.56*	0.29	0.39
LGG	0.08	0.03	–0.15	0.01	–0.20	–0.03
LGS	0.12	0.04	–0.00	0.40	–0.01	0.08
LGSB	0.51**	0.64***	0.39	0.72**	0.56*	0.55*
ORCHIDEE	–0.13	–0.25	–0.16	0.29	–0.10	–0.10

*,**,and *** : Pearson correlation passed the Student's t-test at the 0.1, 0.05, and 0.01 significance level, respectively.

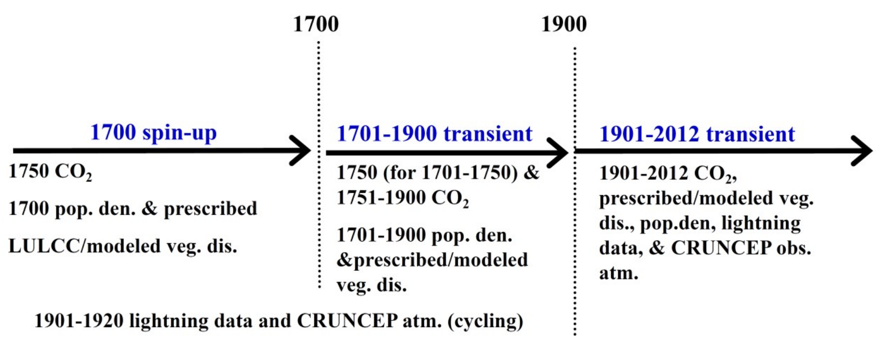

Figure 1. FireMIP experiment design. Note that CTEM and MC2 start at 1861 and 1901 and spin-up using 1861 and 1901 CO2, population density, and prescribed / modeled vegetation distribution, respectively.

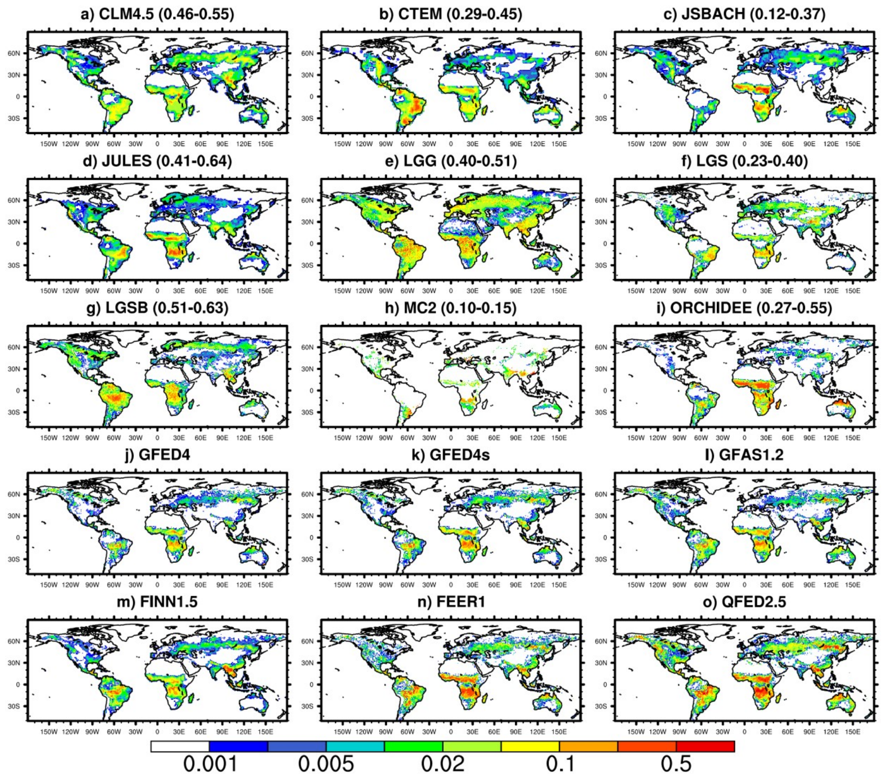

Figure 2. Spatial distribution of annual fire black carbon (BC) emissions (g BC m^{-2} yr^{-1}) averaged over 2003–2008. The range of global spatial correlation between DGVMs and satellite-based products is also given in brackets.

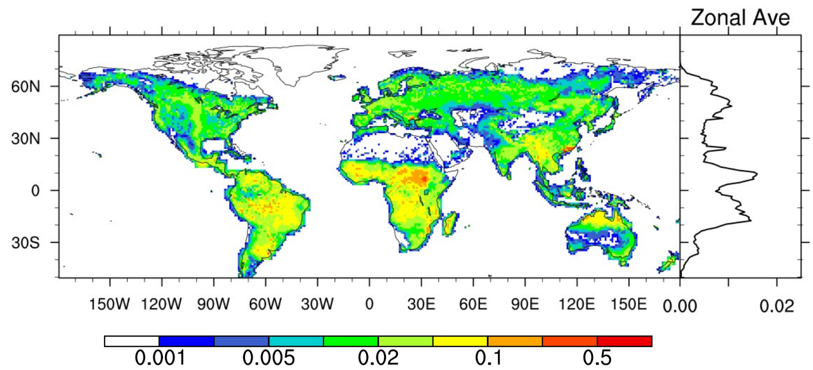

Figure 3. Inter-model standard deviation of 2003–2008 averaged fire BC emissions (g BC m^{-2} yr^{-1}) in FireMIP models and the zonal average.

Atmos. Chem. Phys. Discuss., https://doi.org/10.5194/acp-2019-37
Manuscript under review for journal Atmos. Chem. Phys.
Discussion started: 8 March 2019

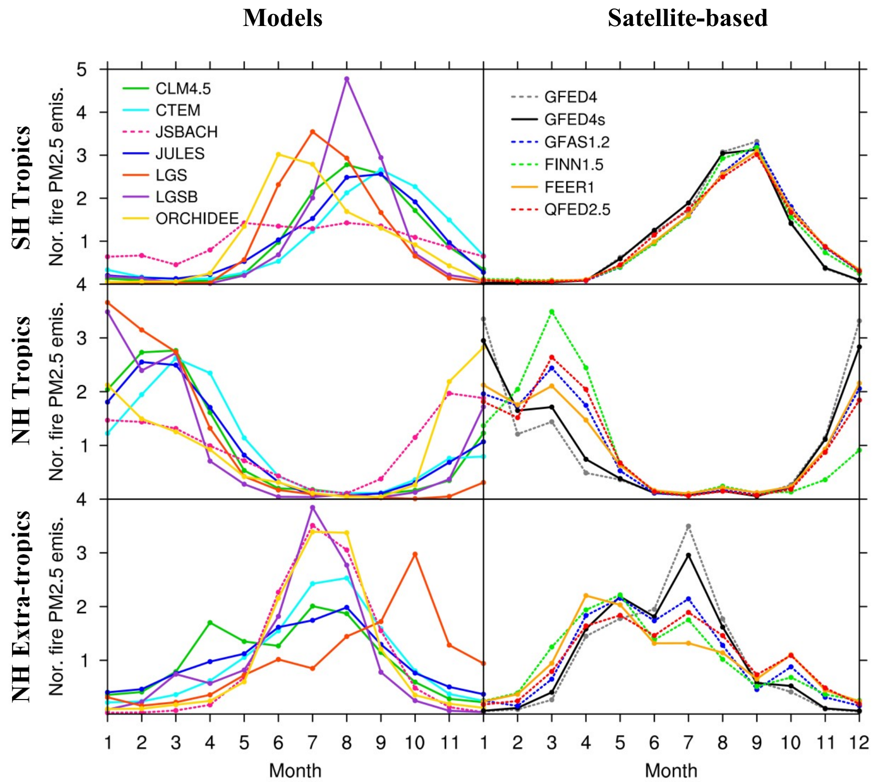

Figure 4. Seasonal cycle of fire $PM_{2.5}$ emissions normalized by the mean from FireMIP models and satellite-based products averaged over 2003–2008 in the Southern Hemisphere (SH) tropics (0–23.5ºS), Northern Hemisphere (NH) tropics (0–23.5ºN), and NH extra-tropics (23.5–90ºN). Fire emissions from LPJ-GUESS-GlobFIRM and MC2 are updated annually and thus are not included here.

Atmos. Chem. Phys. Discuss., https://doi.org/10.5194/acp-2019-37
Manuscript under review for journal Atmos. Chem. Phys.
Discussion started: 8 March 2019

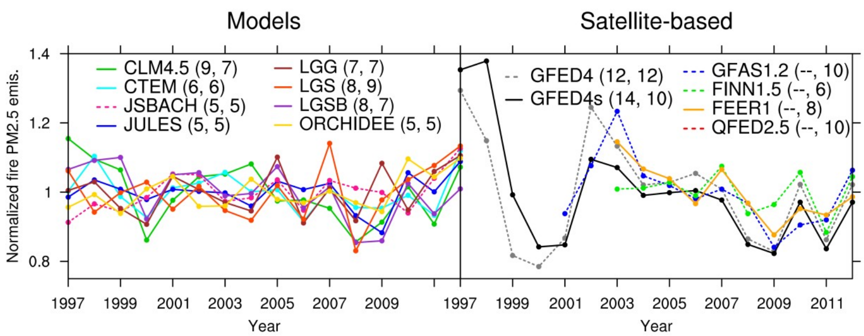

Figure 5. Temporal change of annual global fire $PM_{2.5}$ emissions normalized by the mean from FireMIP models and satellite-based products. The numbers in the brackets are coefficient of variation (CV, the standard deviation divided by the mean, unit: %) for 1997–2012 and 2003–2012, respectively.

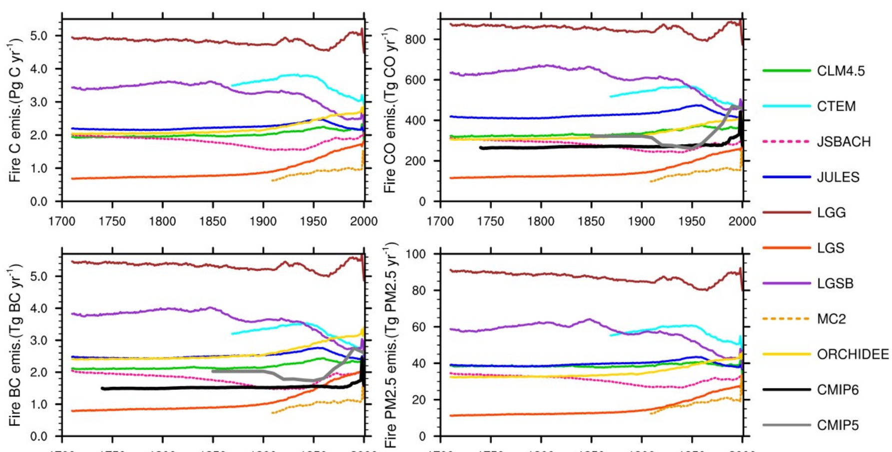

Figure 6. Long-term temporal change of fire emissions from DGVMs in FireMIP and CMIPs forcing. A 21-year running mean is used.

Atmos. Chem. Phys. Discuss., https://doi.org/10.5194/acp-2019-37
Manuscript under review for journal Atmos. Chem. Phys.
Discussion started: 8 March 2019

Atmospheric Chemistry and Physics Discussions

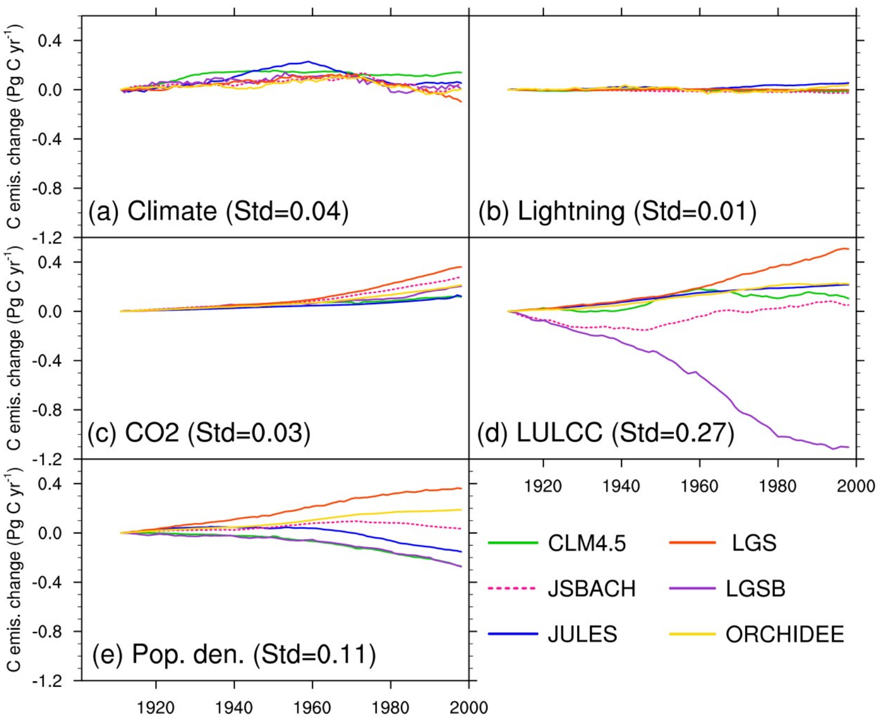

Figure 7. Change in global annual fire carbon emissions (Pg C yr^{-1}) in the 20th century due to changes in (a) climate, (b) lightning frequency, (c) atmospheric CO_2 concentration, (d) land use and land cover change (LULCC), and (e) population density (control run–sensitivity run). A 21-year running mean is used. The standard deviation (Std) of multi-model simulated long-term changes averaged over the 20th century is also given in the bracket.

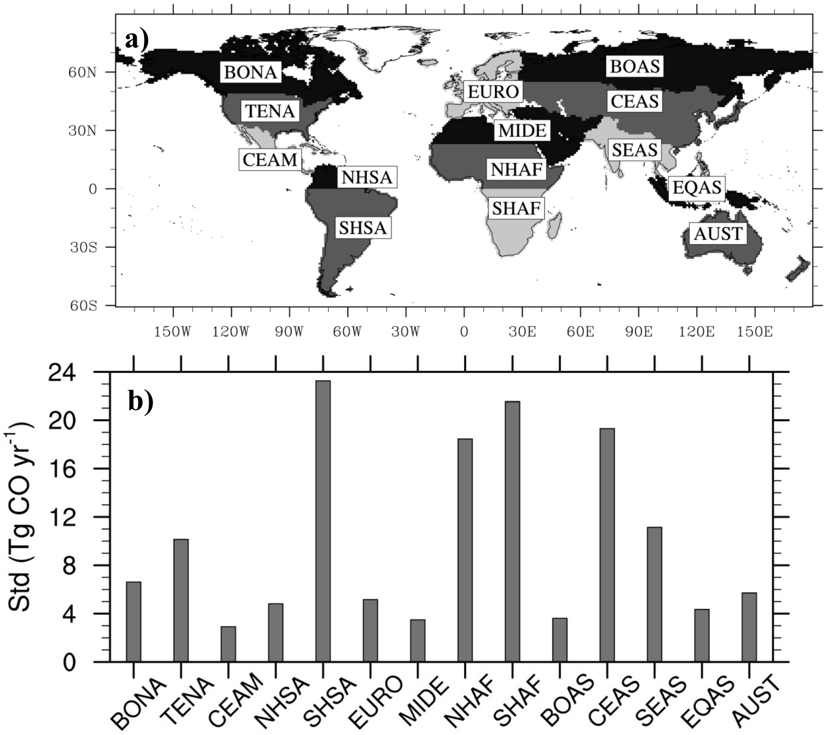

Figure 8. a) GFED region definition (http://www.globalfiredata.org/data.html), and b) inter-model discrepancy (quantified using inter-model standard deviation) in long-term changes (a 21-year running mean is used, relative to present-day) of simulated regional fire CO emissions (Tg CO yr^{-1}) averaged over 1700–2012 (calculate long-term changes relative to present-day for each FireMIP model first, then the inter-model standard deviation, and lastly the time-average). Acronyms are BONA: Boreal North America; TENA: Temperate North America; CEAM: Central America; NHSA: Northern Hem. South America; SHSA: Southern Hem. South America; EURO: Europe; MIDE: Middle East; NHAF: Northern Hem. Africa; SHAF: Southern Hem. Africa; BOAS: Boreal Asia; CEAS: Central Asia; SEAS: South East Asia; EQAS: Equatorial Asia; AUST: Australia.

Atmos. Chem. Phys. Discuss., https://doi.org/10.5194/acp-2019-37
Manuscript under review for journal Atmos. Chem. Phys.
Discussion started: 8 March 2019

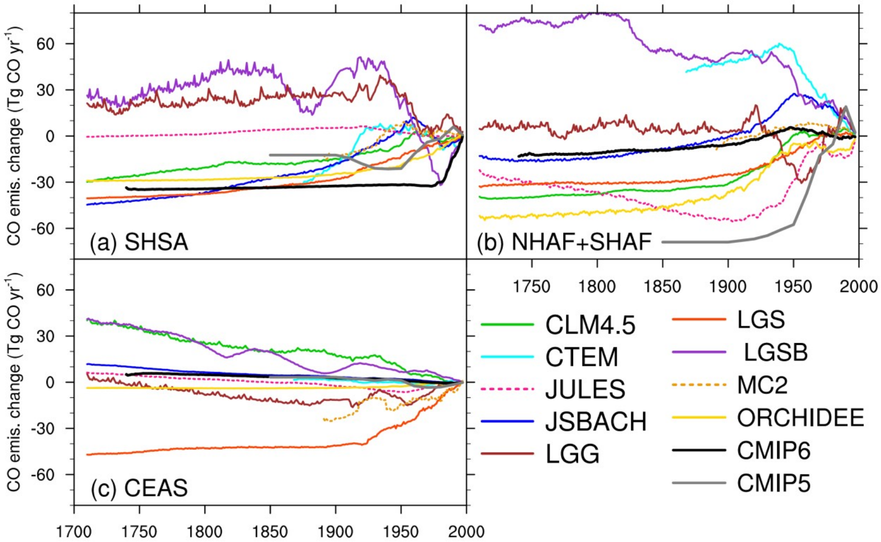

Figure 9. Long-term changes of annual regional fire CO emissions (Tg CO yr^{-1}) from FireMIP models and CMIPs for regions with highest inter-model discrepancy in long-term changes of regional fire emissions shown in Fig. 8. A 21-year running mean is used.